



HAL
open science

Phase shift imaging in thin films using CW Z-scan based technique

Oumar Ba, Mihaela Chis, Christophe Cassagne, Georges Boudebs

► To cite this version:

Oumar Ba, Mihaela Chis, Christophe Cassagne, Georges Boudebs. Phase shift imaging in thin films using CW Z-scan based technique. *Physica B: Condensed Matter*, 2021, 603, pp.412608. 10.1016/j.physb.2020.412608 . hal-03147967

HAL Id: hal-03147967

<https://univ-angers.hal.science/hal-03147967>

Submitted on 3 Feb 2023

HAL is a multi-disciplinary open access archive for the deposit and dissemination of scientific research documents, whether they are published or not. The documents may come from teaching and research institutions in France or abroad, or from public or private research centers.

L'archive ouverte pluridisciplinaire **HAL**, est destinée au dépôt et à la diffusion de documents scientifiques de niveau recherche, publiés ou non, émanant des établissements d'enseignement et de recherche français ou étrangers, des laboratoires publics ou privés.



Distributed under a Creative Commons Attribution - NonCommercial 4.0 International License

Phase shift imaging in thin films using CW Z-scan based technique

Oumar Ba ⁽¹⁾, Mihaela Chis ⁽²⁾, Christophe Cassagne ⁽¹⁾, Georges Boudebs ^(1,*)

⁽¹⁾ *Laboratoire de Photonique d'Angers, LPHIA, EA 4464, SFR MATRIX, UNIV Angers, 2 Boulevard Lavoisier, 49045, Angers, France*

⁽²⁾ *ESAIP, 18, rue du 8 mai 1945 - CS 80022 - 49180 St-Barthélemy d'Anjou Cedex, France*

* *Tel: (33) 2.41.73.54.26, Fax: (33) 2.41.73.52.16, e-mail: georges.boudebs@univ-angers.fr*

ABSTRACT

The beam waist relative variation (BWRV) method known as a Z-scan based technique is used to demonstrate its feasibility in characterizing the thermal effects induced by a continuous laser beam in different materials. A study of several classical solvent-based solutions (water, ethanol, methanol ...) is carried out before introducing the extension of the BWRV method to laterally map the tested sample. We show that the transverse xy-scan of the sample allows to extract an image of the phase shift due to local thermal heating. This new device, called XYZ-scan, is designed for the thermal characterization of inhomogeneous samples. An example will be given on an inhomogeneous 1.6 μm thick thin film doped with silver nanoparticles.

Keywords: Thermo-optical heating, thermal lens, phase shift, Z-scan, linear absorption.

1. INTRODUCTION

Historically, images of objects invisible to the naked eye were necessary in several fields including material science engineering. Particularly, the technique of phase contrast in microscopy has found many applications thanks to its propriety of revealing objects that are transparent. High power laser beam induces temporary phase shifts due to thermal effect in quasi transparent material [1, 2]. Indeed, in high repetition rate laser systems, the responses observed in different materials are highly dependent on cumulative heat in the sample. If the repetition rate is such that the sample does not have time to cool down between two shots the cumulative effect may induce nonlinear (NL) phase shift due to increase in local temperature and can be damaging the tested medium. The dependence of the thermal response of the material is not simple and many studies try to simplify the problem considering only few parameters. Thermal lens effect has been reported in the literature since 1964 [1]. Several studies followed to improve the model, most of which considered the beam as gaussian [3, 4, 5]. Besides, with much higher intensities it is possible to induce phase shifts through the third order NL optical susceptibility. To characterize this phenomenon, the Z-scan technique was first proposed by Sheik-Bahae et al. [6] where the far field diffraction method of the laser beam interacting with the induced phase shift has been simplified. Here the sample is moved with a focused laser beam through its focal region. Information on the magnitude of two-photon absorption and Kerr effect is acquired by analysing the normalized transmission of the sample as a function of its position. It is one of the most popular methods used for the determination of third order and higher NL optical properties due to its simplicity and high sensitivity. Later, the dependence of the far-field intensity on sample position due to intensity-dependent optical nonlinearities has been analysed on the basis of the thermal-lens model of Gordon et al. [7] and the Gaussian decomposition analysis of Sheik-Bahae et al. [8]. The beam waist relative variation (BWRV) method [9] which will be used in this paper is a Z-scan based technique. It has been already successfully applied to measure the Kerr effect using picosecond pulsed laser [10, 11, 12, 13, 14]. The parameters to be measured here in low power CW regime are not due to the Kerr effect but to thermal ones. Indeed, moving the sample around the focal point of the beam will induce a change in the incident intensity and therefore a change in the refractive index of the sample due to increasing thermal effect. This can be exploited to obtain images showing different absorbent objects as chemical species in microbiological samples [15] or in semiconductor optoelectronic components especially when high output power is required [16]...Laser photothermal microscope with coaxial excitation and probe beams was proposed in [15] and application for absolute temperature determination in semiconductor laser diode was performed in [16].

This work begins with a rapid presentation of the BWRV method. We demonstrate its feasibility to characterize the thermal effects induced by a CW beam of a few mW at 532 nm. The contribution of the absorption in a liquid and the linearity of the signal with the power of the incident beam will be investigated using some classical solvents. Then, the method will be extended to transversally scan the sample in the focal region. We demonstrate that this new single beam technique (XYZ-scan) allows to extract an image of the phase shift induced by the local thermal heating. It will be applied to map an inhomogeneous thin film doped with different concentrations of silver nanoparticles.

2. THEORY

2.1 Thermal effect

Following reference [17] in which some assumptions were considered: dimensions of the cell are large compared with the diameter of the beam, heat conduction through the ends can be neglected, and thus the temperature variation can be taken as purely radial. The following symbols will be used: α absorbance in m^{-1} ; ρ density in Kg/m^3 ; I beam intensity; L thickness of the medium (cell) in m ; P beam power in W ; c specific heat in $\text{J}/\text{Kg}/\text{K}$; ω beam radius in m ; ΔT temperature variation in $^\circ\text{K}$; k thermal conductivity in $\text{J}/\text{s}/\text{m}/\text{K}$; λ wavelength in m .

Starting from the heat equation in transient mode, assuming an incident Gaussian beam and taking into account the aberrant nature of the thermal lens [17], the variation in temperature in the medium is given by:

$$\Delta T(r, t) = \frac{2P\alpha}{\pi c\rho\omega^2} \int_0^t \left(\frac{1}{1+2t'/t_c} \right) \exp\left(\frac{-2r^2/\omega^2}{1+2t'/t_c} \right) dt', \quad (1)$$

where $t_c = \omega^2 c\rho/4k$. This temperature variation induces a change in the linear index according to the following relationship:

$$\Delta n(r, t) = \frac{dn}{dT} \Delta T(r, t), \quad (2)$$

with dn/dT denoting the thermo-optical coefficient. The induced phase shift is related to Δn as usual using $\Delta\varphi = 2\pi\Delta nL/\lambda$.

2.2 Characterization method

The next step is to determine what effect this refractive-index distribution has on the beam intensity at the output of a 4f imaging system. The experimental setup used to implement the BWRV is presented in Fig. 1. We recall here briefly the method; more experimental details can be found in [10, 11, 12].

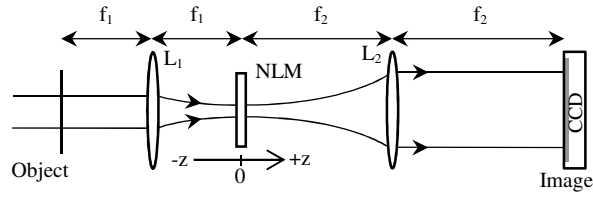


Fig. 1. Experimental setup. The sample (NLM) is scanned along the beam direction around the focal plane ($z=0$). The labels refer to: lenses (L_1 and L_2) and Camera (CCD).

This setup is composed of an afocal imaging system ($f_1 = 10 \text{ cm}$; $f_2 = 20 \text{ cm}$) so that the magnification is equal to 2. The sample under investigations is moved along the beam direction in the focus region. An image of the output beam, transmitted by the sample, is then recorded by a CCD camera. It has been shown in [10, 11] that the signal, $\Delta\omega_{pv}$ which is the difference between the peak and the valley (see Fig. 2-a) is a linear function of the peak induced effective phase shift $\Delta\phi_0$ (defined at the center of the beam) and at the focus ($z = 0$) ($\Delta\omega_{pv} = 0.3\Delta\phi_0$). The laser is a CW Nd:YAG type emitting at 532 nm. At the laser output, a polarizing system ($\lambda/2 + \text{GLAN}$) (not visible in Fig. 1) allows the incident power to be varied from 0 to $\approx 15 \text{ mW}$. Then, a spatial filter is placed to clean and to expand the beam. The output beam irradiates the object plane at the input of the afocal imaging system. The first lens (L_1) focuses the light on the sample (NLM) with a beam waist approximately equal to $18 \mu\text{m}$. The NLM can move around the common focal plane of both lenses L_1 and L_2 . Then, the image of the output beam is formed on the CCD sensor thanks to L_2 . The dimensional variation in the transmitted beam profiles are directly related to the induced phase-shifts in the NLM. The evolution of the BWRV, calculated using the first and second moment of the recorded spatial beam intensity distribution, is then calculated versus the position z of the sample. Two sets of acquisitions are performed for each measurement. The first set is done in the high-power regime and the second in the low-power one; this is necessary to remove from the measurements the diffraction, diffusion and/or imperfection due to the inhomogeneity of the sample. For all subsequent acquisitions, 0.465 mm pitch is used on the z axis, for a total displacement of 28.365 mm . This gives 61 images per scan and 122 images for a complete acquisition (low and high power). The exposure times range from 100 ms to 2 s . Taking into account the characteristic time (t_c) of our samples it is considered that the acquisitions are carried out in the stationary regime. Indeed, the CCD camera has a relatively long response time and does not allow to study time dependence for rapid transient regimes. Moreover, a minimum delay time of 0.5 s between each acquisition is necessary to move the motor and to dampen the generated mechanical vibrations. Tests were performed at different integration times of the CCD (0.25s , 0.5s , 0.75s and 1s) and the

results clearly showed that the generated signals were very close validating the steady state induced phase shift measurements.

3. RESULTS AND DISCUSSIONS

3.1 Checking the linearity of the signal

In the first place, the feasibility of the experiment has been achieved with the study of a basic solvent (methanol) to which we have progressively added Indian ink as absorbing pigment at different concentrations under different incident laser beam power. In Fig. 2(a), we show two BWRV profiles corresponding to pure methanol and to a few drops of ink dissolved in methanol characterized by an absorption coefficient: $\alpha = 5.2 \times 10^{-5} m^{-1}$. The signal $\Delta\omega_{pv}$ is the difference between the maximum and the minimum of the profile.

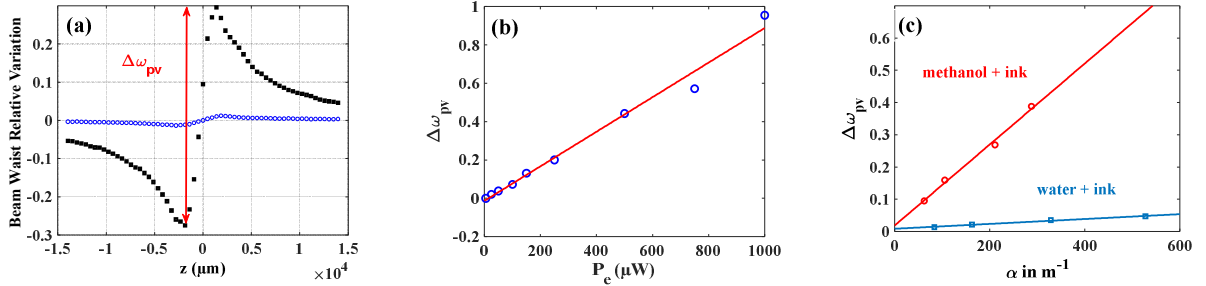


Fig. 2. (a) BWRV profiles of pure methanol (blue circles) and methanol with ink (black squares) for the same beam power ($P_e = 700 \mu W$, $L = 2 mm$); the vertical arrow shows the signal: $\Delta\omega_{pv}$. (b) Evolution of the signal as a function of the laser beam power for a fixed concentration in ethanol. (c) Evolution of $\Delta\omega_{pv}$ versus α , the linear absorption characterizing different concentrations of ink diluted in methanol (red circles) and ink diluted in water (blue squares) for a fixed input power (2 mW). Solid lines in (b) and (c) are the linear regression lines.

It is well known that the thermal effect contributes to a negative phase shift related to a negative variation of the refractive index. This change is due to a decrease in density with the increase of temperature. In contrary to classical open aperture Z-scan, the signature of the BWRV showing a minimum followed by a maximum is typical of a negative Δn . Comparing the two profiles, notice the 30 times higher response of methanol with ink inducing higher $\Delta\omega_{pv}$ which indicates a larger variation in the refractive index due to a higher absorption inside the liquid. The question that remains is whether our signal $\Delta\omega_{pv}$ is linear as a function of the input power for a given concentration. In Fig. 2 (b), we highlight the evolution of this response showing the predicted linearity on a large scale using ethanol as a solvent. To show the effect of the concentration and the solvent thermo-optical characteristics on the signal, measurements were taken using two solutions: ink with distilled water and ink with methanol at different concentrations. We gradually diluted the solutions and reported in Fig. 2 (c) the measured $\Delta\omega_{pv}$ corresponding to each absorption value α , with an incident power P_e of 2 mW and a cell of 1 mm

thickness. Of course, we notice the linear response as a function of the absorption, which is in accordance with the theoretical equations developed in [7]. Note the difference in the slope of the solid regression lines when the solvent changes, due to the different thermo-optical coefficients. Indeed, for the same ink concentration the solvent induces different index variations (different $\Delta\omega_{pv}$) according to its different thermal parameters such as the specific heat, the thermal conductivity and the density.

3.2 Transversal sample mapping

We have described the BWRV method which makes it possible to obtain the induced phase from a Z-scan over one point of a sample. This phase shift $\Delta\varphi_0$ allows us to find the refractive index Δn . After this, a scanning system is added in the focal plane orthogonal to the optical axis z over which the scan is made. Three translation plate were separately motorized covering xyz axes and controlled by three controllers (Fig. 3 (a)). These plates allow 30 mm translation for each axis with a step (resolution) of 1.25 μm . Connected to the computer, the translation system is driven by a LABVIEW program. A Z-scan is made for each coordinate point (x_i, y_i) to find the index variation of the material at that point. A restitution of all these measurements would give a thermo-optical image of the solid thin film sample. This process is called XYZ-scan, it is very useful for studying inhomogeneous materials in terms of density, absorption...

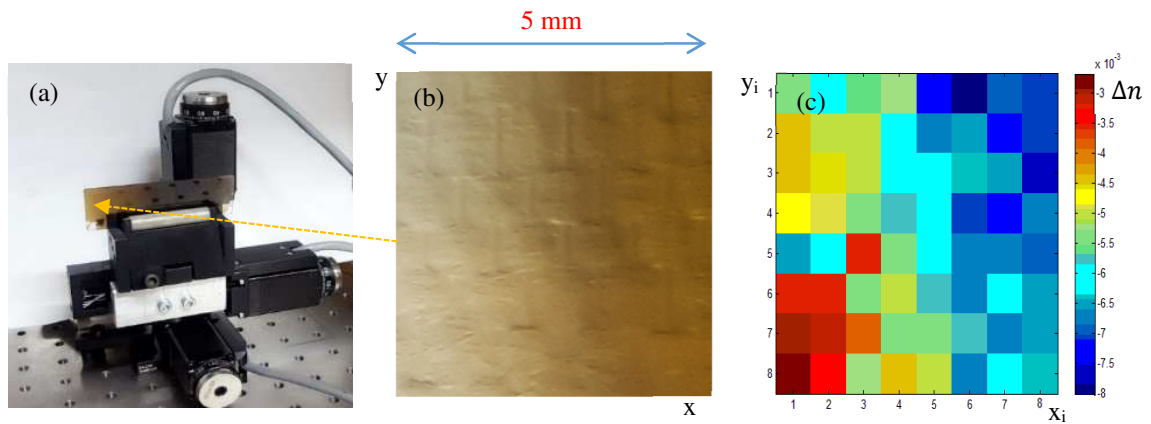


Fig. 3: (a) The thin film on the tri-axis translation plate. (b) image of the thin film 1.6 μm thick ($\text{SiO}_2\text{-TiO}_2 + \text{Ag}$) shown in (a); (c) cartography of the thermal effects and the measured Δn ($-8 \times 10^{-3} < \Delta n < -3 \times 10^{-3}$) for $P_e = 7.5$ mW. Acquisition and processing time 20 mn for 64 measurement points.

To validate our method, the studied sample was an inhomogeneous thin sol-gel film of $\text{SiO}_2\text{TiO}_2 + \text{Ag}$ ($10^{-3}M$) (Fig. 3(b)) with a thickness of 1.6 μm deposited on a microscope glass slide. The film was exposed to a 7.5 mW continuous laser beam. 64 measurement points (Fig. 3(c)) were carried out over an area covering $5 \times 5 \text{ mm}^2$. This area was divided into 8x8 equidistant squares on the edge of the film where the inhomogeneity

appears to the naked eye. As the acquisition time is 4 min for each point (more than 4 hours was needed to obtain the final image), it was useful to reduce the scan interval travel over z near the minimum and the maximum found in the BWRV signal. This brought us to a total acquisition time of 20 minutes.

The heterogeneity of the film can be easily distinguished by looking at the measured values from Δn which are correlated to the visible light transmission of the film. Fig. 3(c) shows in red points the lowest absolute values of Δn which fits the lower left side of the film as shown in Figure 3(b) where it is bright. Since the laser power is the same for all the acquisitions over all the considered points, one can check that the higher variation of Δn is related to the higher concentration of doping metallic Ag nanoparticles in the film.

According to reference [15] using coaxial excitation and probe beams, the spatial resolution of the thermal lens microscope is determined by the spot size of the excitation beam and was less susceptible to the thermal diffusion length. In fact, the probe beam in [15] had approximately the same spatial extension as the excitation one. Thus, in theory, when dealing with single-beam techniques, the final image can have a spatial resolution of the same order of magnitude as conventional linear imaging systems, since the variation in index is related to the variation in intensity profile in the focal plane, which in the best case has a dimension close to the micrometer. Here the excitation beam ($\omega = 18 \mu m$) is far from that ideal case using high numerical aperture microscope objective but the purpose of the paper is to demonstrate the feasibility of extracting this phase shift image with only one beam. Evidently, the spatial resolution will also depend on the time it takes to obtain the final image which is related to the number of dots per millimeter square to be measured, the power of the computer, the efficiency of the software and the smallest step of the motor used for transverse-scanning...

Concerning the contrast, it is related to the evolution of the BWRV response showing the predicted linear relation with the induced phase shift. Fig. 2 (b) shows an example of how large the scale of the response could be. We estimated to a maximum of 100% (BWRV=1) the relative variation of the beam dimension where the signal remains linear with the absorption. This value corresponds to a phase shift of $\Delta\varphi_H = \pi$. Tests have been done to estimate the minimum detectable signal to be around 3×10^{-3} , which corresponds to $\Delta\varphi_L = 10 \text{ mrad}$. The contrast of the images should then be $C = (\Delta\varphi_H - \Delta\varphi_L) / (\Delta\varphi_H + \Delta\varphi_L) \approx 0.99$ which is theoretically very close to the maximum value that one can obtain in imaging systems.

CONCLUSION

In summary, it is possible to construct new types of images due to thermal effects induced by heating the doping impurities in transparent thin films irradiated with a low power CW laser beam using a single beam technique. The beam waist relative variation (BWRV) method at the output of an imaging system has been successfully applied to demonstrate the feasibility of quantifying the measurable coefficients that allow for retrieving these images. For this purpose, we have experimentally demonstrated the linearity between the measured signal and the incident laser power as well as the concentration in some weakly absorbing solutions. The obtained steady signals with a CCD are not sensitive to the characteristic time for the transient induced nonlinear index variation. Otherwise, this paper also aims to draw attention to the possible confusions that some researchers may have by associating the relatively slow thermal responses obtained with a low power continuous mode laser generating induced phase shifts due to absorption with that of instantaneous Kerr induced phase shifts using high intensity pulsed lasers.

Acknowledgements

The authors would like to acknowledge the financial support from the NNN-TELECOM Program, Région des Pays de la Loire, contract n°: 2015 09036.

REFERENCES

- [1] J. P. Gordon, R. C. C. Leite, R. S. Moore, S. P. S. Porto, and J. R. Whinnery, *J. Applied. Physics.* 36, 3 (1965).
- [2] Khurgin, J. B., Sun, G., Chen, W. T., Tsai, W. Y., & Tsai, D. P. Ultrafast thermal nonlinearity. *Scientific Reports*, 5, 17899 (2015).
- [3] Hu, C., & Whinnery, J. R., New thermo-optical measurement method and a comparison with other methods. *Applied Optics*, 12(1), 72-79. (1973).
- [4] Whinnery, J. R., Laser measurement of optical absorption in liquids. *Accounts of Chemical Research*, 7(7), 225-231 (1974).
- [5] Carman, R. L., and P. L. Kelley. "Time dependence in the thermal blooming of laser beams." *Applied Physics Letters* 12.8: 241-243 (1968).
- [6] Sheik-Bahae, M., Said, A. A., Wei, T. H., Hagan, D. J., & Van Stryland, E. W. Sensitive measurement of optical nonlinearities using a single beam. *IEEE journal of quantum electronics*, 26(4), 760-769 (1990).
- [7] Gordon, J. P., Leite, R. C. C., Moore, R., Porto, S. P. S., & Whinnery, J. R. Long-transient effects in lasers with inserted liquid samples. *Journal of Applied Physics*, 36(1), 3-8 (1965).
- [8] Cuppo, F. L. S. A., Neto, A. M. F., Gómez, S. L., & Palffy-Muhoray, P. Thermal-lens model compared with the Sheik-Bahae formalism in interpreting Z-scan experiments on lyotropic liquid crystals. *JOSA B*, 19(6), 1342-1348 (2002).
- [9] Boudebs, G., Besse, V., Cassagne, C., Leblond, H., & de Araújo, C. B. Nonlinear characterization of materials using the D4 σ method inside a Z-scan 4f-system. *Optics letters*, 38(13), 2206-2208 (2013).
- [10] G. Boudebs, V. Besse, C. Cassagne, H. Leblond, and Cid B. de Araújo, "Nonlinear characterization of materials using the D4 σ method inside a Z-scan 4f-system" *Optic Letters*, 38, 13, 2206-2208, (2013).
- [11] De Araújo, Cid B., Anderson SL Gomes, and Georges Boudebs. "Techniques for nonlinear optical characterization of materials: a review." *Reports on Progress in Physics* 79.3: 036401 (2016).
- [12] Wang, H., Boudebs, G., & de Araújo, C. B. "Picosecond cubic and quintic nonlinearity of lithium niobate at 532 nm". *Journal of Applied Physics*, 122(8), 083103, (2017).
- [13] Derkowska-Zielinska, B., Barwiolek, M., Cassagne, C., & Boudebs, G., "Nonlinear optical study of Schiff bases using Z-scan technique". *Optics & Laser Technology*, 124, 105968. (2020).

- [14] Boudebs, G., Wang, H., Cassagne, C., Chis, M., Amaral, A. M., & de Araújo, C. B., "Influence of strong light beams on the nonlinear refraction and absorption coefficients of transparent materials". *JOSA B*, 36(12), 3411-3416, (2019)
- [15] Uchiyama, K., Hibara, A., Kimura, H., Sawada, T., & Kitamori, T., "Thermal lens microscope", *Japanese Journal of Applied Physics*, 39(9R), 5316, (2000).
- [16] Mansanares, A. M., Roger, J. P., Fournier, D., & Boccara, A. C., « Temperature field determination of InGaAsP/InP lasers by photothermal microscopy: Evidence for weak nonradiative processes at the facets », *Applied physics letters*, 64(1), 4-6, (1994).
- [17] Sheldon, S. J., L. V. Knight, and J. M. Thorne. "Laser-induced thermal lens effect: a new theoretical model." *Applied optics* 21.9: 1663-1669 (1982).